



LAWRENCE  
LIVERMORE  
NATIONAL  
LABORATORY

# Electrospray mass spectrometry of NeuAc oligomers associated with the C fragment of the tetanus toxin

M. C. Prieto, R. M. Whittal, M. A. Baldwin, A. L.  
Burlingame, R. Balhorn

April 5, 2005

Journal of the American Society for Mass Spectrometry

## **Disclaimer**

---

This document was prepared as an account of work sponsored by an agency of the United States Government. Neither the United States Government nor the University of California nor any of their employees, makes any warranty, express or implied, or assumes any legal liability or responsibility for the accuracy, completeness, or usefulness of any information, apparatus, product, or process disclosed, or represents that its use would not infringe privately owned rights. Reference herein to any specific commercial product, process, or service by trade name, trademark, manufacturer, or otherwise, does not necessarily constitute or imply its endorsement, recommendation, or favoring by the United States Government or the University of California. The views and opinions of authors expressed herein do not necessarily state or reflect those of the United States Government or the University of California, and shall not be used for advertising or product endorsement purposes.

# **Electrospray mass spectrometry of NeuAc oligomers associated with the C fragment of the tetanus toxin**

Maria C. Prieto\*

Chemistry and Materials Science Directorate, Lawrence Livermore National Laboratory,  
Livermore, CA 94550

Randy M. Whittal<sup>‡</sup>, Michael A. Baldwin, A. L. Burlingame

Mass Spectrometry Facility, Department of Pharmaceutical Chemistry, University of California,  
San Francisco, CA 94143-0446

Rod Balhorn

Biology and Biotechnology Research Program, Lawrence Livermore National Laboratory,  
Livermore, CA 94550

Running title: Protein.carbohydrate  $K_D$ 's from ESI-MS

Address reprint requests to Dr. Balhorn, Biology and Biotechnology Research Program,  
Lawrence Livermore National Laboratory, Livermore, CA 94550, (925)422-6284, FAX  
(925)422-2282 email address: balhorn2@llnl.gov

\* Present address: Thermo Electron Corp., San Jose, CA 95134, (408)965-6018

<sup>‡</sup> Present address: Department of Chemistry, University of Alberta, Edmonton, Alberta,  
T6G 2G2, Canada (780)492-5577

---

The *Clostridial* neurotoxins, botulinum and tetanus, gain entry into neuronal cells by protein recognition involving cell specific binding sites. The sialic or N-acetylneuraminic acid (NeuAc) residues of gangliosides attached to the surface of motor neurons are the suspected recognition and interaction points with *Clostridial* neurotoxins, although not necessarily the only ones. We have used electrospray ionization mass spectrometry (ESI-MS) to examine formation of complexes between the tetanus toxin C fragment, or targeting domain, and carbohydrates containing NeuAc groups to determine how NeuAc residues contribute to ganglioside binding. ESI-MS was used to rapidly and efficiently measure dissociation constants for a number of related NeuAc-containing carbohydrates and NeuAc oligomers, information that has helped identify the structural features of gangliosides that determine their binding to tetanus toxin. The strength of the interactions between the C fragment and (NeuAc)<sub>n</sub>, are consistent with the topography of the targeting domain of tetanus toxin and the nature of its carbohydrate binding sites. The results suggest that the targeting domain of tetanus toxin contains two binding sites that can accommodate NeuAc (or a dimer). This study also shows that NeuAc must play an important role in ganglioside binding and molecular recognition, a process critical for normal cell function and one frequently exploited by toxins, bacteria and viruses to facilitate their entrance into cells.

---

---

Both botulinum and tetanus neurotoxins interact with motor neurons, blocking acetylcholine release and causing muscle paralysis and death (for an excellent review, see Neimann, 1991, [1]). The first step required for toxin entrance into neurons is the

recognition of gangliosides at the cell surface by the receptor-binding domain of the heavy chain [2]. Following the binding of the toxin to the cell surface, an endosome forms and the translocation domain of the toxin transfers the catalytic domain, a zinc protease, into the cell. Once inside the cell, the protease cleaves one of three specific proteins involved in neurotransmitter release, depending on the toxin type.

The targeting domain of the tetanus toxin has been identified as the 51 kDa carboxy-terminal peptide of the heavy chain [3], called the C fragment. Although there is considerable evidence indicating that gangliosides are cell surface receptors targeted by this domain, gangliosides may not be the only receptors. It has also been suggested that a protein receptor may be required for efficient binding of this toxin to the neuron [4]. The protein receptor has not yet been identified. In certain cases, such as the botulinum neurotoxin, different serotypes may exhibit a preference for different types of gangliosides or protein receptors. The strongest and hence most specific ganglioside association with the tetanus toxin occurs with  $G_{T1b}$ , a trisialo sphingolipid with a branched carbohydrate structure containing a single NeuAc on one arm and a NeuAc dimer on the other (Table 1).

Some of the first successful analyses of biomolecules by ESI-MS were reported by Fenn et al. in 1989 [5], building upon techniques developed in earlier work by Dole et al. (1968). ESI-MS enables the introduction of liquid samples into a mass spectrometer, thereby allowing the analysis of highly polar and nonvolatile biological compounds [6]. Non-specific aggregates of proteins in ESI-MS, such as those induced by salt or high protein concentrations, were first reported in the late 1980's. The ability to measure specific non-covalent interactions by ESI-MS was soon established [7],[8]. Reviews of

the study of non-covalent interactions by ESI-MS have been published by Loo (1997), Smith et al. (1997) and Last and Robinson (1999). The properties of ESI-MS make it an ideal technique for rapid determinations of stoichiometry and dissociation constants, especially when solution methods prove difficult [9] or little analyte is available.

In a previous study we used ESI-MS to screen a group of ligands to identify those that bind to the tetanus toxin C-fragment. The molecules tested were predicted to bind by screening a ligand database using computational docking tools and assessing their ability to form a complex with the tetanus toxin C fragment [10]. In the present work, we show that ESI-MS can be used to measure equilibrium dissociation constants (equation 2, below) between the C fragment and NeuAc-containing carbohydrates. Dissociation constants were measured for a series of NeuAc oligomers, (NeuAc)<sub>n</sub>, n=1 to 6, to assess the validity of the technique for discerning small changes in binding strengths. The ESI-MS results are compared to published results for ganglioside binding obtained by other solution-based techniques to identify the features of a ganglioside structure that contribute to its binding to tetanus neurotoxin.

## **Experimental**

### *Materials*

A recombinant form of the tetanus toxin C fragment was purchased from Roche Molecular Biochemicals/Boehringer Mannheim (USA). The NeuAc monomer (309.3 Da), and the oligomeric dimer (644.5 Da), trimer (957.7 Da), tetramer (1271 Da), pentamer (1584.2 Da), and hexamer (1897.5 Da), were obtained from Calbiochem-Novabiochem Corp. (La Jolla, CA) as the sodium salts.  $\beta$ D-Gal(1-3)D-GalNAc (383.4 Da) and the sodium salts of oligosaccharides occurring in the gangliosides GM<sub>3</sub> and

GT<sub>1b</sub>, 3'-N-acetylneuraminyl lactose (3'-sialyllactose, 655.5 Da), di-N-acetylneuraminyl lactose (disialyllactose, 963.7 Da) were purchased from Sigma Chemical Co. (St. Louis, MO). These compounds were used without further purification.

#### *Sample treatment and complex formation*

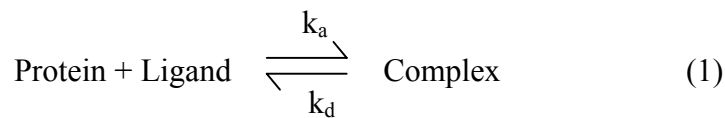
The tetanus C fragment (recombinant and purified by acid precipitation) was dissolved in filtered deionized water (18 Mohm cm<sup>-1</sup>, Millipore) and centrifuged to remove the insoluble residue that forms at pH<9. Aliquots of the supernatant were hydrolyzed in HCl and the protein concentration was determined by quantitative amino acid analysis (Protein Structure Laboratory, University of California, Davis, CA). UV-VIS absorption measurements were used to accurately determine the protein concentration in each experiment. In the binding experiments protein concentration was kept constant, while the ligand concentration was varied. Twenty microliter samples were prepared for analysis. The C fragment sample was diluted to a final concentration of 3-13 μM in 3 mM aqueous ammonium acetate (pH ~7.6) and 12% methanol. Stock carbohydrate samples were dissolved in water and final dilutions were made in 3 mM aqueous ammonium acetate (pH ~7.6) and 12% methanol. No attempt was made to remove the Na<sup>+</sup> salts from the carbohydrates by dialysis.

#### *Instrumentation*

Samples were analyzed by ESI-MS on a Mariner orthogonal acceleration time-of-flight (oa-TOF) instrument (Applied Biosystems, Framingham MA). The use of this instrument to monitor non-covalent interactions has been described before (R.M. Whittal, H.L. Ball, F.E. Cohen, A.L. Burlingame, S.B. Prusiner, and M.A. Baldwin. *Protein Sci.* 9, 332

(2000). R. M. Whittal, C. C. Benz, G. Scott, J. Semyonov, A. L. Burlingame, and M. A. Baldwin. *Biochemistry* 39, 8406 (2000). The singly and doubly charged ions of Gramicidin S were used to calibrate the mass scale, typically at the start of each day. Freshly mixed protein/carbohydrate samples were introduced by infusion from a syringe pump through fused silica capillaries (60 and 25  $\mu\text{m}$  ID) at 1  $\mu\text{L}/\text{min}$ . Once a stable signal was obtained, spectra were accumulated over a period of 2 min. All spectra were acquired at room temperature to minimize dissociation of the complexes. Instrument settings, such as gas flow rates, number of scans, spray tip potential, and declustering or nozzle potentials were optimized and kept constant for each set of experiments corresponding to a specific complex. The nozzle or declustering potential was adjusted in the range 50-300 V to obtain a qualitative estimate of the strength and nature of the non-covalent interactions. Multiply charged spectra were deconvoluted using the Biospec Data Explorer software supplied with the mass spectrometer.

### *Data analysis*



$$K_D = \frac{k_d}{k_a} = \frac{[\text{Protein}][\text{Ligand}]}{[\text{Complex}]} \quad (2)$$

Equation 1 describes the equilibrium between free protein and free ligand in solution and the complex, where  $k_a$  and  $k_d$  are rate constants for the formation and breakdown of the



complex respectively. Equation 2 expresses the equilibrium constant  $K_D$  for dissociation of the complex in terms of concentration. All experiments were carried out with a fixed concentration of protein and a varying concentration of carbohydrate. Assuming that ion peak intensities in an ESI mass spectrum are proportional to solution concentrations, and assuming the formation of a single complex, the ratio  $[\text{Protein}]/[\text{Complex}]$  can be derived from the ratio of the peak heights for the protein alone and the protein.carbohydrate complex. The dissociation constant can be derived from a plot of this ratio vs.  $1/[\text{ligand}]$  [9].

## **Results and Discussion**

### *Electrospray MS of the Tetanus Toxin C- fragment*

Figure 1 is a typical ESI-MS spectrum of the tetanus toxin C fragment, showing the monomer protein envelope (M) and a dimer (2M). The mass deconvolution spectra for these two peaks (Figure 2) yield masses of 51,819 and 103,606 for the protein M and 2M components, respectively. The molecular weight of this recombinant protein is 51,758 Da (Protein Data Bank, 1A8D). The observed differences in mass between the molecular weights derived from the protein sequence and our measured values (61 Da for the monomer, 90 Da for the dimer) are small and appear to be attributed to tightly bound counterions (acetate, ammonium, sodium) or water molecules.

*Specificity of dimer formation* Using this protein, we investigated the effects of varying the protein concentration (Fig. 3, 4) and the organic solvent content (Fig.5) on the ion abundance, mass accuracy, and mass spectrum appearance in order to determine if dimer formation (2M) is specific, and perhaps biologically relevant, or simply a consequence of self aggregation. Random aggregation is often observed in proteins at higher

concentrations. Denaturing the protein would be expected to disturb or eliminate dimerization if specific inter-molecular interactions contribute to the formation or stabilize the dimer complex [11]. The electrospray interface conditions were also varied in an attempt to disrupt the weak binding forces that occur in non-covalent interactions. Because associations that occur as a consequence of the electrospray process, high analyte concentrations, or protein unfolding (denaturation) are not physiologically significant, it is important that they be minimized. The ionization response factor of protein monomer over dimer was also not taken into account, since we compared relative peak heights.

Samples run at a declustering potential of 300 V provided the best signal to noise (S/N) and highest resolution spectra for the C-fragment ( $m/dm=216$  at 300 V). This is the highest and most stable declustering potential we could apply with the Mariner instrument. The ion abundance ratio obtained for the protein (monomer : dimer) is plotted in Fig. 3 as a function of protein concentration. The monomer is approximately five times more abundant than the dimer at 300 V, and this ratio remains constant with increasing protein concentration. In contrast, the ratio of monomer to dimer decreases with increasing protein concentration when the samples are run at 200 V. A lower ion abundance is also observed, in general, for the dimer peak in runs conducted at 200 V. Evaporation of the solvent and fragmentation of the electrosprayed droplet ultimately cause the creation of ions by charge repulsion. Higher ion abundance is documented when counterions are efficiently knocked off during this process, an event which occurs at higher voltages, especially at the gentle instrumental conditions used to detect non-

covalent complexes in our samples. Voltages were varied in the same electrosprayed sample.

A deterioration in the quality of the mass spectrum (peak width increase and signal to noise (S/N) decrease) is observed at C fragment concentrations  $>15 \mu\text{M}$  (M, data not shown) and 200 V declustering voltage. The S/N does not degrade when working at 300V. The loss of resolution may explain why lower mass values than expected are recorded at  $30\mu\text{M}$  (M, 200 V) and  $\geq 10 \mu\text{M}$  (2M, 200 V) (Fig. 4 data table). An increase in mass values was, for the most part, the trend observed as the protein concentration increased for both M and 2M peaks and at both 200 and 300 V (Fig. 4 data table). Salts and contaminants present with the protein would also increase at higher protein concentrations. The low resolution of the Mariner instrument at this high molecular weight did not provide an exact mass difference that could be attributed to the addition of  $\text{NH}_4^+$ ,  $\text{Na}^+$ , or acetate ions. The mass ratio M/2M was observed to be exactly 0.5 for most protein concentrations when the samples were run at a skimmer voltage of 300 V, instead of 200 V (Fig. 4), indicating that the 2M peak is exactly double the mass of the M peak. This is consistent with the concept that adducted ions should be more efficiently dissociated at a potential of 300 V compared to 200 V.

Low amounts of methanol were added to samples to improve the efficiency of the electrospray ionization. Increasing the methanol concentration did not appear to affect the protein M envelope distribution, however the protein 2M peak disappeared from the mass spectrum when the methanol concentration reached 40% (Fig. 5). This result suggests that the interactions that stabilize dimer formation may be disrupted by moderate methanol concentrations. The degradation in S/N of the dimer peak occurs gradually as

the concentration of MeOH increases, while the monomer only shows a decrease in S/N at 40% MeOH (Fig. 5b).

The presence of the C-fragment dimer at various protein concentrations, specifically at the low concentrations, and the loss of the dimer signal at 40% methanol, suggest that the dimer exists in solution and is not an artifact produced by the electrospray process. This is consistent with native gel electrophoresis and chemical crosslinking experiments which have also indicated tetanus neurotoxin forms dimers and trimers in solution [12]. The observation that the dimer withstands high skimmer voltages suggests that the interaction is probably electrostatic in nature. The C fragment of tetanus toxin corresponds to the toxin's targeting domain, which once bound to the cell receptor, participates in forming channels or pores [13]; [14]; [15]; [16]. Consequently, we would expect the C fragment to be able to bind specifically not only to receptors on the surface of the cell, but to each other as well. While we did not observe trimers or tetramers due to the mass range limitations of the Mariner instrument, previous electron cryomicroscopy [16] and ion conductance [15] studies have indicated that both botulinum and the closely related tetanus neurotoxins probably interact as tetramers to form channels in neuronal membranes.

#### *Characterization of the C fragment/ligand complexes*

Figure 6 (a, b) shows a typical ESI-MS spectrum after mass deconvolution in which both the unbound and ligand-bound protein peaks are resolved. All the ligands tested for binding are listed in Table 2, along with the experimentally determined dissociation constants measured at declustering voltages in the range of 200 to 300 V. Figure 7 shows a plot and linear regression of equation 2 for the C fragment -(NeuAc)<sub>3</sub> complex. The

dissociation constant for this ligand,  $33\mu\text{M}$ , is obtained from the slope of the line. Since proteins of comparable sizes have been shown to have similar ionization response factors in ESI-MS [17]; [18], we expect the ionizability of the protein and the protein-complex to be similar in these experiments. Nevertheless, only ion abundances from the same spectrum were compared in each experiment.

Samples were prepared with low ligand to protein ratios to ensure the formation of specific complexes and minimize non specific interactions (clustering or aggregation). Saturation binding curves were generated for each ligand to determine the working concentration range. The amount of bound protein (normalized to unbound protein) increased linearly, in proportion to ligand concentration, up to a saturation point. Increasing the ligand concentration beyond this point did not produce any more bound protein and an asymptote was reached (data not shown). In each experiment, the ligand concentration was kept within the linear region of the saturation binding curve [19]. Notice that the inverse parameters are plotted for dissociation constant determination following equation 2, compare axis labels for Fig. 7.

All the NeuAc-containing ligands formed strong associations with the C fragment in the gas phase that withstood dissociation at high declustering voltages (200-300 V), indicating that the complexes were primarily stabilized by electrostatic interactions [11]. The experimental control,  $\beta\text{D-Gal}(1-3)\text{D-GalNAc}$ , the terminal carbohydrate in the ganglioside  $\text{G}_{\text{M1}}$  that lacks a NeuAc group, did not form a complex as determined by ESI-MS. Complexes (normalized to unbound protein) were observed to be most abundant at a skimmer voltage of approximately 200 V (data not shown). Inspection of the low mass region gave an indication of the amount of unbound ligand remaining. The lowest

abundance of free ligand in the mass spectrum was observed at skimmer voltages of 150-200 V, and the concentration of unbound ligand increased with increase in skimmer voltage, suggesting that the majority of the ligand remained bound to the C-fragment at ~200 V. This is consistent with the idea that an increase in the number of collisions between ions and background neutral gases might favor products other than the toxin-ligand complex [18]. The measured dissociation constant from linear plots of Equation 2 was observed to increase slightly (weaker association) with increase in declustering voltage (data not shown). This trend has been previously observed and was attributed, in a triple quadrupole MS, to increased collision-induced dissociation of the complex ions at higher tube lens voltages [18].

#### *Role of Acetylneuraminic Acid in Carbohydrate Binding to Tetanus Toxin*

The  $k_{\text{dissociation}}$  of the NeuAc-containing carbohydrates fell within the 11 to 33  $\mu\text{M}$  range (column 3, Table 2). The ESI-MS technique seems to be sufficiently sensitive to be able to discriminate between structurally related ligands based on the nature of their interaction with the C-fragment. Deconvolution (Biospec Data Explorer software, Applied Biosystems) of two of the data sets, the hexamer and disialyllactose binding, was not possible due to poor S/N of the spectra. The dissociation constants from the deconvoluted data agree with those from the unprocessed data, when both are available (data not shown).

The dissociation constant of the C fragment complex with sialyllactose (NeuAc ( $\alpha$ 2-3)Gal ( $\beta$ 1-4)Glc) and that of the monomer NeuAc were found to be very close in value. A very similar dissociation constant, 10 $\mu\text{M}$ , was reported previously for the binding of the GM<sub>3</sub> ganglioside to the tetanus toxin C fragment in an assay that monitored the

inhibition of C-fragment binding to brain membranes [20]. The dissociation constant of the C fragment bound to disialyllactose ( $23\mu\text{M}$ ), with two NeuAc residues, and that of the dimer NeuAc-NeuAc ( $21\mu\text{M}$ ) were also found to be similar. In addition to demonstrating that two-fold differences in binding affinity can be observed using this approach and may prove to be significant, the results also suggest the presence of the second NeuAc residue may destabilize the interaction of the first residue with a particular binding site, resulting in a slightly higher dissociation constant.

The largest dissociation constants were documented for C-fragment complexes involving the trimer and pentamer (see below for binding of tetramer and hexamer) of NeuAc, indicating that longer oligomers were not as tightly bound to the C-fragment. While these differences in binding affinity are subtle, the general trend observed for the set of NeuAc oligomers appear consistent with both the molecular structure of the gangliosides and the location of sites on BoNT/B (*Clostridium botulinum* neurotoxin type B) and the C-fragment of tetanus toxin where NeuAc residues appear to bind. The complex carbohydrates in the gangliosides that preferentially bind to the clostridial neurotoxins (GT1b, GD1b) contain a single di NeuAc separated from another NeuAc (or two di NeuAc separated from each other) by Gal( $\beta$ 1-3)-GalNAc( $\beta$ 1-4)-Gal (Table 1). Two different NeuAc binding sites have been observed by X-ray diffraction. Crystallographic data obtained by Swaminathan and Eswaramoorthy [21] have shown that the NeuAc residue in sialyllactose binds in a cleft on the surface of the targeting domain of BoNT/B between Trp 1261 and His 1240, one of the potential ganglioside binding sites. A different site has been reported for NeuAc binding on the equivalent domain of tetanus neurotoxin, located near residues 1226 and 1229 [22]. Recent

competition experiments performed using NMR (Cosman et al., manuscript in preparation) have also revealed that sialic acid effectively competes with doxorubicin for binding to the pocket between Trp 1289 and His 1271.

These results, combined with the information that the single NeuAc and the di NeuAc residues are separated by three galactose residues in GT1b (and GD1b, Table 1), suggest that ganglioside binding may involve two adjacent sites on the surface of the targeting domain of the clostridial neurotoxins. If this is true, then one might expect the binding affinities of a series of NeuAc oligomers to reflect the distance between these two binding pockets. Our mass spectrometry results appear to be consistent with this hypothesis. If we consider, for example, the binding of the first NeuAc of GT1b or GD1b into one of the two binding pockets, the distance between this residue and the next NeuAc (or di NeuAc) binding in the second pocket would correspond to  $\sim 25\text{\AA}$  (based on the distance between the NeuAc residues in a ganglioside). This is very close to the distance that separates the two sites on the Clostridial neurotoxin targeting domains that have been identified to bind NeuAc [22] and either sialyllactose [21] or an analog of the GT1b carbohydrate [23]. By analogy, if the NeuAc oligomers bound to these two sites, we would expect the strongest binding to be observed with the monomer and the hexamer. This agrees with the measured binding trend found in our work. While the monomer has a dissociation constant of  $13\mu\text{M}$ , the dimer, trimer, and pentamer bind less tightly. Once the length reached six residues, the binding affinity was observed to increase again. Tetramer binding, which appears to be more complex (two slopes were observed with non deconvolved spectra, on two separate experiments), does not follow the linear premise of this model. This may indicate that tetramer binding to the C-



fragment may occur via an entirely different mode, one that reflects the ability of the tetramer to adopt a unique conformation not attainable by the other oligomers.

The complex formed between the tetanus toxin C-fragment and NeuAc also differed from the binding observed for the NeuAc multimers. This was the only case in which the complex contained a more abundant bound than unbound protein peak in the mass spectrum prior to the binding of a second ligand. The unbound protein peak was always more intense with all the other ligands, regardless of the binding ratio. This would be expected for those ligands with stronger binding affinities, such as the monomer. However, it was not observed with the hexamer, which exhibits a similar affinity for the C fragment.

As the ratio of ligand to protein was increased, a second ligand was observed to bind in each of the NeuAc multimers below the hexamer. A complex containing two NeuAc hexamers would have appeared at a mass that could not be adequately separated from the next charged state of the C-fragment, therefore it was not observed. Similarly, a second pentamer ligand was not observed to bind either. However, the deconvolved spectra of the bound pentamer shows the binding of a second ligand of approximately half its mass (data not shown). This smaller ligand, which we have not been able to identify, is probably a contaminant present in the pentamer. These results provide additional support for the idea that the sialic acids may bind to two different sites on the C-fragment's surface.

The protein to ligand binding ratio at which binding of the second ligand was observed was 1:5 for the monomer, dimer, and trimer, and 1:3 for the tetramer. It is interesting that a second NeuAc residue would bind preferentially to the protein

molecules that already had one NeuAc bound in the presence of so much uncomplexed protein. This is characteristic of ligands that bind in a cooperative manner.

Previous studies have clearly shown that the C fragment of tetanus toxin preferentially binds gangliosides of the series  $G_{T1b}$ ,  $G_{Q1b}$ ,  $G_{D1b}$ . The  $(\text{NeuAc})_2$  group on the internal Gal of this ganglioside series (Table 1) has been reported to be required for binding, as well as the NeuAc on the terminal Gal( $\beta$ 1-3)-GalNAc moiety [24]; [25]. The single NeuAc in the internal Gal, as in  $G_{M1}$ , did not appear to be sufficient for binding using a microtiter assay [24], but it was observed to bind in competition experiments [25]. The NeuAc on the terminal Gal in  $G_{M3}$ , appeared to enhance binding only slightly and was not considered essential for binding [24]. Our ESI-MS experiments, on the other hand, demonstrated that both sialyllactose ( $\text{NeuAc } (\alpha$ 2-3) $\text{Gal } (\beta$ 1-4) $\text{Glc}$ ) and disialyllactose ( $\text{NeuAc } (\alpha$ 2-8) $\text{NeuAc } (\alpha$ 2-3) $\text{Gal } (\beta$ 1-4) $\text{Glc}$ ) bind to the tetanus toxin C fragment. The most likely explanation for the observed differences in binding is that the mass spectrometry technique (and competition assays) can be used to detect weakly bound ligands with micromolar or lower dissociation constants. Such weak binding would not be detected using a microtiter assay because low affinity ligands would dissociate and be removed in the washing steps.

The strength of the interaction between the tetanus toxin and gangliosides reported in the literature also vary widely. Early studies reported the affinities between tetanus toxin and gangliosides to be in the low micromolar range [26]. It was shown later that gangliosides compete for tetanus toxin binding to bovine cerebral cortex membranes with nanomolar potency [20]. A recent study using a quartz crystal microbalance measured binding constants  $k_a$  similar to  $10^6 \text{ M}^{-1}$  between tetanus C fragment and gangliosides

(G<sub>D1a</sub>, G<sub>D1b</sub>, and G<sub>T1b</sub>) on solid supported membranes [27]. Another study using surface plasmon resonance and a liposome capture method obtained dissociation constants for G<sub>D1b</sub> and G<sub>T1b</sub> and the C fragment of 0.15 and 0.17  $\mu$ M, respectively [28].

The dissociation constant measured for disialyllactose in our study is about 100 times weaker than that reported for G<sub>T1b</sub> [28]. This result is consistent with the observation that the additional NeuAc ( $\alpha$ 2-3)Gal( $\beta$ 1-3)-GalNAc residue present in G<sub>T1b</sub> is important to produce a stronger and more specific binding. Other interactions, such as those that might occur between the protein and the lipid bilayer, may explain why nanomolar affinities were measured when binding of tetanus toxin to cerebral membranes was considered [20]. The membrane bilayer plays an important role in specific protein-carbohydrate interactions. The fluidity of the bilayer allows congregation of gangliosides and correct geometric positioning of their polar headgroups [29]; [30]. The monovalent interactions in protein-carbohydrate binding, which can be characterized by unusually low affinities, usually become strong interactions through multivalency that arise from the simultaneous association of two or more proteins and receptors. In fact, using model phosphatidylcholine host membranes, twenty gangliosides per tetanus toxin were reported to be necessary to form a stable pore on the surface [31]. However, gangliosides attached to cellular membranes might be bulkier molecules than previously thought, so twenty gangliosides at the membrane surface might be too large of a structure.

A recent X-ray crystallography study [22] showed that four separate carbohydrates: NeuAc, galactose, lactose, and N-acetylgalactosamine, bind to different sites of the C fragment. Interestingly, a single NeuAc was found to bind in the region of residues 1226 to 1229, adjacent to the position occupied by N-acetylgalactosamine in a separate crystal

structure. Their results support the hypothesis that the C fragment contains multiple carbohydrate binding sites.

The conformation of the NeuAc oligomers tested for binding to the C-fragment was not given much consideration in this study, primarily because it has been widely documented that both ligands and the proteins they bind readily change conformation upon binding. Capillary electrophoresis of NeuAc polymers have recently shown that oligomers containing two to five units migrate in reverse order according to their molecular masses [32]. This was attributed in part to a large degree of heterogeneity found in the conformation of  $\alpha$ -2,8-linked NeuAc oligomers. Smaller oligomers move randomly in an electric field while polymers larger than six units start forming rod-like structures and migrate in a predictable manner. In contrast to carbohydrate oligomers in solution, the oligosaccharide groups in gangliosides embedded in membranes seem to extend well beyond the bilayer surface with a well defined average conformation and motional order [30]. For this reason, the interaction between toxin and gangliosides in the cell is usually expected to be fairly specific.

The validity of using this electrospray technique to measure dissociation constants between *Clostridial* neurotoxins and their receptors has recently been confirmed in another study [10]. Doxorubicin, a ligand that was found to bind to the C fragment, produced a dissociation constant of 11  $\mu$ M by the same electrospray technique used in this work. The complex could be dissociated in the gas phase by increasing the skimmer voltage, indicating that the association was possibly more hydrophobic in character than the interaction with NeuAcs. A competitive assay using ganglioside-bearing liposomes

produced a dissociation constant with a very similar value of 9.4  $\mu\text{M}$  for this complex [10].

## **Conclusion**

Electrospray ionization MS has been successfully used to examine complex formation between the targeting domain of tetanus toxin and a set of NeuAc containing ligands in a rapid and unambiguous manner. The dissociation constant measured for sialyllactose using ESI MS, which was very close to that obtained previously by other methods, provides evidence that this type of complex maintains its structural integrity in the gas phase. The dissociation constant obtained for disialyllactose was determined to be substantially weaker than the binding constant measured previously for  $G_{T1b}$ , which suggests that the terminal NeuAc( $\alpha$ 2-3)Gal( $\beta$ 1-3)-GalNAc in  $G_{T1b}$  (and possibly interactions with other protein toxin sites and/or among the carbohydrates) impart both greater specificity and higher affinity. The consistency in values obtained in our study reaffirms ESI-MS as a valuable technique in the study of specific, non-covalent interactions between proteins and ligands. The strength of the interactions between the C fragment and  $(\text{NeuAc})_n$ , is consistent with the topography of the targeting domain of tetanus toxin and the nature of its carbohydrate binding sites. The results suggest that the targeting domain of tetanus toxin contains two binding sites that can accommodate NeuAc (or a dimer), separated by a distance of  $\sim 25\text{\AA}$  (an estimate obtained from the crystal structure of the C-fragment structure). This is consistent with the structure of  $G_{T1b}$  and related gangliosides that bind to the tetanus toxin targeting domain. The NeuAc residues in these branched carbohydrates are separated by a similar distance.

**Acknowledgements:**

The mass spectrometry work at UCSF was supported by NIH NCRR BRTP Grant RR01614. The work conducted at Lawrence Livermore National Laboratory was supported by the Department of Energy's Chemical and Biological Non-Proliferation Program. R.M.W. thanks the Natural Sciences and Engineering Research Council of Canada for the postdoctoral fellowship. M.C.P. thanks Professor Ronald Schnaar and his group (Johns Hopkins University) for stimulating discussions and helpful suggestions. This work was performed under the auspices of the U.S. Department of Energy by UC, Lawrence Livermore National Laboratory under Contract W-7405-ENG-48.

## References:

1. Montecucco, C.; Schiavo, G. Structure and function of tetanus and botulinum neurotoxins *Quarterly Reviews of Biophysics* **1995**, *28*, 423-472.
2. Williamson, L. C.; Bateman, K. E.; Clifford, J. C. M.; Neale, E. A. Neuronal sensitivity to tetanus toxin requires gangliosides *J. Biol. Chem.* **1999**, *274*, 25173-25180.
3. Shapiro, R. E.; Specht, C. D.; Collins, B. E.; Woods, A. S.; Cotter, R. J.; Schnaar, R. L. Identification of a ganglioside recognition domain of tetanus toxin using a novel ganglioside photoaffinity ligand *J. Biol. Chem.* **1997**, *272*, 30380-30386.
4. Schengrund, C. L. What is the cell surface receptor(s) for the different serotypes of botulinum neurotoxin? *J. Toxicol.-Toxin Rev.* **1999**, *18*, 35-44.
5. Fenn, J. B.; Mann, M.; Meng, C. K.; Wong, S. F.; Whitehouse, C. M. Electrospray Ionization for Mass-Spectrometry of Large Biomolecules *Science* **1989**, *246*, 64-71.
6. Gaskell, S. J. Electrospray: Principles and practice *J. Mass Spectrom.* **1997**, *32*, 677-688.
7. Ganem, B.; Li, Y. T.; Henion, J. D. Detection of Noncovalent Receptor Ligand Complexes by Mass- Spectrometry *J. Am. Chem. Soc.* **1991**, *113*, 6294-6296.
8. Katta, V.; Chait, B. T. Observation of the Heme Globin Complex in Native Myoglobin by Electrospray-Ionization Mass-Spectrometry *J. Am. Chem. Soc.* **1991**, *113*, 8534-8535.

9. Greig, M. J.; Gaus, H.; Cummins, L. L.; Sasmor, H.; Griffey, R. H. Measurement of Macromolecular Binding Using Electrospray Mass- Spectrometry - Determination of Dissociation-Constants for Oligonucleotide-Serum Albumin Complexes *J. Am. Chem. Soc.* **1995**, *117*, 10765-10766.
10. Lightstone, F. C.; Prieto, M. C.; Singh, A. K.; Piqueras, M. C.; Whittal, R. M.; Knapp, M. S.; Balhorn, R.; Roe, D. C. Identification of novel small molecule ligands that bind to tetanus toxin *Chem. Res. Toxicol.* **2000**, *13*, 356-362.
11. Smith, R. D.; Bruce, J. E.; Wu, Q. Y.; Lei, Q. P. New mass spectrometric methods for the study of noncovalent associations of biopolymers *Chem. Soc. Rev.* **1997**, *26*, 191-202.
12. Ledoux, D. N.; Be, X. H.; Singh, B. R. Quaternary Structure of Botulinum and Tetanus Neurotoxins as Probed by Chemical Cross-Linking and Native Gel-Electrophoresis *Toxicon* **1994**, *32*, 1095-1104.
13. Hoch, D. H.; Romeromira, M.; Ehrlich, B. E.; Finkelstein, A.; Dasgupta, B. R.; Simpson, L. L. Channels Formed by Botulinum, Tetanus, and Diphtheria Toxins in Planar Lipid Bilayers - Relevance to Translocation of Proteins across Membranes *Proceedings of the National Academy of Sciences of the United States of America Biophys* **1985**, *82*, 1692-1696.
14. Gambale, F.; Montal, M. Characterization of the Channel Properties of Tetanus Toxin in Planar Lipid Bilayers *Biophys. J.* **1988**, *53*, 771-783.
15. Montal, M. S.; Blewitt, R.; Tomich, J. M.; Montal, M. Identification of an Ion Channel-Forming Motif in the Primary Structure of Tetanus and Botulinum Neurotoxins *FEBS Lett.* **1992**, *313*, 12-18.



16. Schmid, M. F.; Robinson, J. P.; Dasgupta, B. R. Direct Visualization of Botulinum Neurotoxin-Induced Channels in Phospholipid-Vesicles *Nature* **1993**, *364*, 827-830.
17. Vandorsselaer, A.; Bitsch, F.; Green, B.; Jarvis, S.; Lepage, P.; Bischoff, R.; Kolbe, H. V. J.; Roitsch, C. Application of Electrospray Mass-Spectrometry to the Characterization of Recombinant Proteins up to 44 Kda *Biomedical and Environmental Mass Spectrometry* **1990**, *19*, 692-704.
18. Jorgensen, T. J. D.; Roepstorff, P.; Heck, A. J. R. Direct determination of solution binding constants for noncovalent complexes between bacterial cell wall peptide analogues and vancomycin group antibiotics by electrospray ionization mass spectrometry *Anal. Chem.* **1998**, *70*, 4427-4432.
19. Lim, H. K.; Hsieh, Y. L.; Ganem, B.; Henion, J. Recognition of Cell-Wall Peptide Ligands by Vancomycin Group Antibiotics - Studies Using Ion-Spray Mass-Spectrometry *Journal of Mass Spectrometry* **1995**, *30*, 708-714.
20. Rogers, T. B.; Snyder, S. H. High-Affinity Binding of Tetanus Toxin to Mammalian Brain Membranes *J. Biol. Chem.* **1981**, *256*, 2402-2407.
21. Swaminathan, S.; Eswaramoorthy, S. Structural analysis of the catalytic and binding sites of Clostridium botulinum neurotoxin B *Nat. Struct. Biol.* **2000**, *7*, 693-699.
22. Emsley, P.; Fotinou, C.; Black, I.; Fairweather, N. F.; Charles, I. G.; Watts, C.; Hewitt, E.; Isaacs, N. W. The structures of the H-C fragment of tetanus toxin with carbohydrate subunit complexes provide insight into ganglioside binding *J. Biol. Chem.* **2000**, *275*, 8889-8894.

23. Fotinou, C.; Emsley, P.; Black, I.; Ando, H.; Ishida, H.; Kiso,; Sinha, K.A.; Fairweather, N.F.; Isaacs, N.W. The crystal structure of tetanus toxin Hc fragment complexed with a synthetic GT1b analog suggests crosslinking between ganglioside receptors and the toxin. *J. Biol. Chem* **2001**, *276*, 32274-32281.
24. Angstrom, J.; Teneberg, S.; Karlsson, K. A. Delineation and Comparison of Ganglioside-Binding Epitopes for the Toxins of Vibrio-Cholerae, Escherichia-Coli, and Clostridium-Tetani - Evidence for Overlapping Epitopes *Proc. Natl. Acad. Sci. U. S. A.* **1994**, *91*, 11859-11863.
25. Holmgren, J.; Elwing, H.; Fredman, P.; Svennerholm, L. Polystyrene-Adsorbed Gangliosides for Investigation of the Structure of the Tetanus-Toxin Receptor *Eur. J. Biochem.* **1980**, *106*, 371-379.
26. Ledley, F. D.; Lee, G.; Kohn, L. D.; Habig, W. H.; Hardegree, M. C. Tetanus Toxin Interactions with Thyroid Plasma-Membranes - Implications for Structure and Function of Tetanus Toxin Receptors and Potential Pathophysiological Significance *J. Biol. Chem.* **1977**, *252*, 4049-4055, Lee, G.; Grollman, E. F.; Dyer, S.; Beguinot, F.; Kohn, L. D.; Habig, W. H.; Hardegree, M. C. Tetanus Toxin and Thyrotropin Interactions with Rat-Brain Membrane Preparations *J. Biol. Chem.* **1979**, *254*, 3826-3832.
27. Janshoff, A.; Steinem, C.; Sieber, M.; elBaya, A.; Schmidt, M. A.; Galla, H. J. Quartz crystal microbalance investigation of the interaction of bacterial toxins with ganglioside containing solid supported membranes *Eur. Biophys. J. Biophys. Lett.* **1997**, *26*, 261-270.

28. MacKenzie, C. R.; Hirama, T.; Lee, K. K.; Altman, E.; Young, N. M. Quantitative analysis of bacterial toxin affinity and specificity for glycolipid receptors by surface plasmon resonance *J. Biol. Chem.* **1997**, *272*, 5533-5538.
29. Evans, S. V.; MacKenzie, C. R. Characterization of protein-glycolipid recognition at the membrane bilayer *J. Mol. Recognit.* **1999**, *12*, 155-168.
30. Brocca, P.; Sonnino, S. Dynamics and spatial organization of surface gangliosides *Trends Glycosci. Glycotechnol.* **1997**, *9*, 433-445.
31. Winter, A.; Ulrich, W. P.; Wetterich, F.; Weller, U.; Galla, H. J. Gangliosides in phospholipid bilayer membranes: Interaction with tetanus toxin *Chem. Phys. Lipids* **1996**, *81*, 21-34.
32. Kakehi, K.; Kinoshita, M.; Hayase, S.; Oda, Y. Capillary electrophoresis of N-acetylneuraminic acid polymers and hyaluronic acid: Correlation between migration order reversal and biological functions. *Analytical Chemistry* **1999**, *71*, 1592-1596.

Table 1. Ganglioside structures. Carbohydrate sections tested for binding to the tetanus C fragment appear in bold.

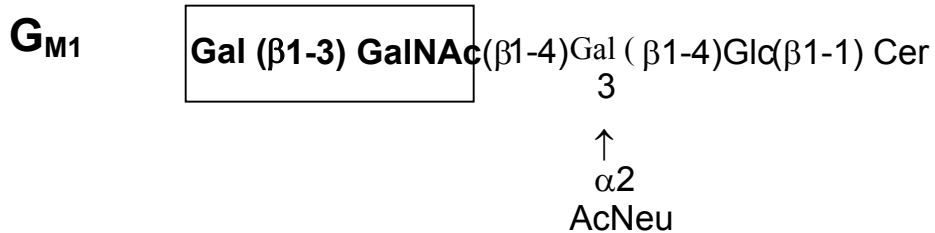
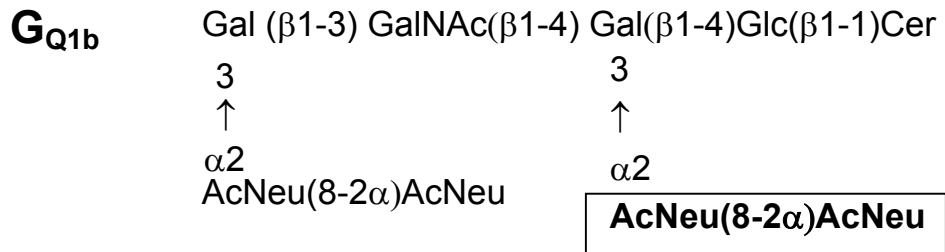
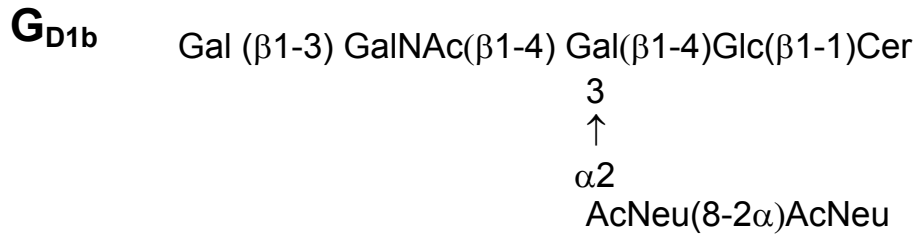
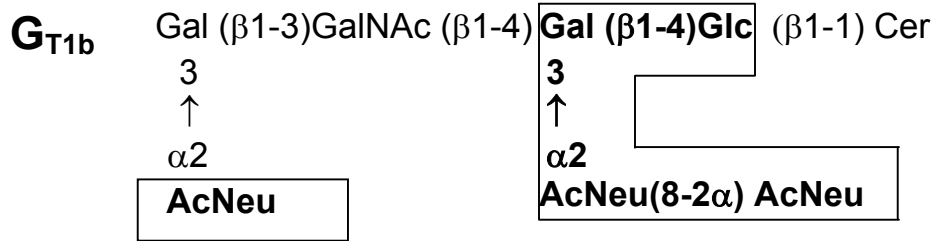


Table 2. Ligands tested for noncovalent complex formation with the tetanus C fragment. Spectra were deconvoluted, unless noted otherwise. The standard error was obtained from regression analysis using Microsoft Excel.

<b>Carbohydrate</b>	<b>Declustering Voltage</b>	<b>K<sub>dissociation</sub> (μM)</b>
NeuAc	<b>200V</b>	<b>13 ± 2<sup>a</sup></b>
	<b>250V</b>	<b>15 ± 2</b>
(NeuAc) <sub>2</sub>	<b>200V</b>	<b>21 ± 4</b>
(NeuAc) <sub>3</sub>	<b>200V</b>	<b>33 ± 4</b>
(NeuAc) <sub>4</sub>	<b>200V</b>	<b>12 ± 2<sup>b</sup></b>
(NeuAc) <sub>5</sub>	<b>200V</b>	<b>23 ± 3</b>
(NeuAc) <sub>6</sub>	<b>200V</b>	<b>11 ± 4<sup>a</sup></b>
<i>Sialyllactose</i> (G <sub>M3</sub> section; one NeuAc acid)	<b>200V</b>	<b>11 ± 2</b>
<i>Disialyllactose</i> (G <sub>T1b</sub> section; two NeuAc acids)	<b>200V</b>	<b>23 ± 5<sup>a</sup></b>
Ganglioside control: β-D-Gal(α1-3)GalNAc	<b>50-250V</b> <b>(declustering voltages tested)</b>	<b>No binding</b>

NeuAc=sialic acid

**a** spectra not deconvoluted. Note that when available, data from both raw data and deconvoluted spectra were in good agreement.

**b** average of two separate binding experiments gave similar results.

Figure 1. ESI MS spectrum from 7  $\mu$ M solution of the C fragment protein, recorded with a declustering voltage of 300 V, showing the monomer (M) multiply charged envelope with  $z$  equal to 17, 16, 15 and 14, and the dimer (2M) at higher  $m/z$  with  $z$  equal to 24, 23, 22 and 21.

Figure 2. Deconvolution of separate regions of the ESI MS spectra of the tetanus C fragment, corresponding to a) M, and b) 2M.

Figure 3. C fragment concentration vs. ion abundance of M/2M at declustering voltages of 200 and 300 V.

Figure 4. Variation in the M/2M ratio of observed mass values after deconvolution, plotted against increasing C fragment concentration, at declustering voltages of a) 200 V and b) 300 V.

Figure 5. ESI MS spectra of the tetanus C fragment in, a) 10% methanol, showing both M and 2M peaks, and b) 40% methanol, showing the disappearance of the 2M peak. The protein concentration was 8.6  $\mu$ M in 3 mM ammonium acetate, pH 7.5. The declustering voltage was 200 V in both cases.

Figure 6. Deconvoluted spectra recorded with a declustering voltage of 200 V, showing complex formation between the C fragment and NeuAc dimers and trimers. a) Top trace,

1:4 C fragment : (NeuAc)<sub>2</sub>, bottom trace, 1:8 C fragment : (NeuAc)<sub>2</sub>. b) Top trace, 1:3 C fragment : (NeuAc)<sub>3</sub>; bottom trace, 1:7 C fragment : (NeuAc)<sub>3</sub>.

Figure 7. Binding of (NeuAc)<sub>3</sub> to the C fragment. The dissociation constant  $K_D$  is derived from the slope of the plot of the ratio of unbound C fragment/bound C fragment vs.  $1/[(\text{NeuAc})_3]$  (see equation 2).

Table 1. Ganglioside structures. Carbohydrate sections tested for binding to the tetanus C fragment appear in bold.

Table 2. Ligands tested for noncovalent complex formation with the tetanus C fragment. Spectra were deconvoluted, unless noted otherwise. The standard error was obtained from regression analysis using Microsoft Excel.

**a** spectra not deconvoluted. Note that when available, data from both raw data and deconvoluted spectra were in good agreement.

**b** average of two separate binding experiments gave similar results.

Figure 1. ESI MS spectrum from 7  $\mu$ M solution of the C fragment protein, recorded with a declustering voltage of 300 V, showing the monomer (M) multiply charged envelope with z equal to 17, 16, 15 and 14, and the dimer (2M) at higher m/z with z equal to 24, 23, 22 and 21.

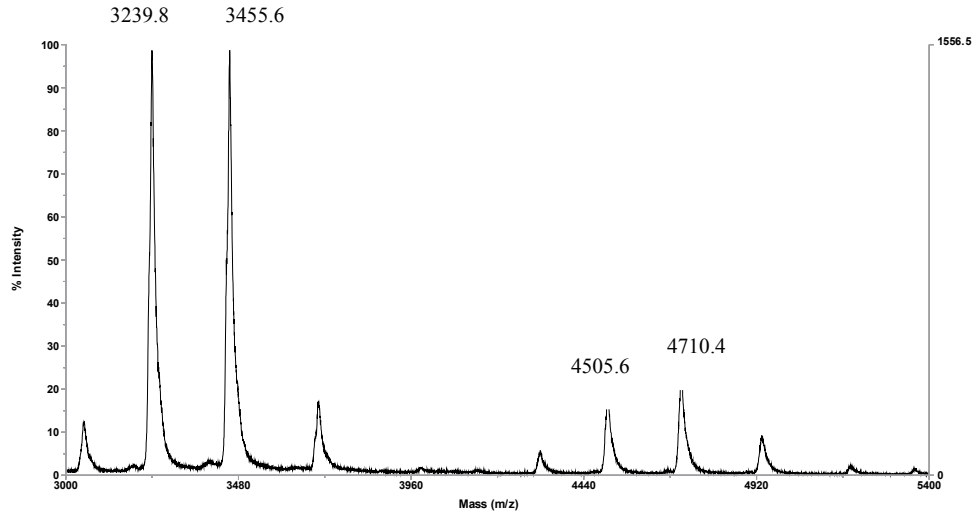




Figure 2. Deconvolution of separate regions of the ESI MS spectra of the tetanus C fragment, corresponding to a) M, and b) 2M.

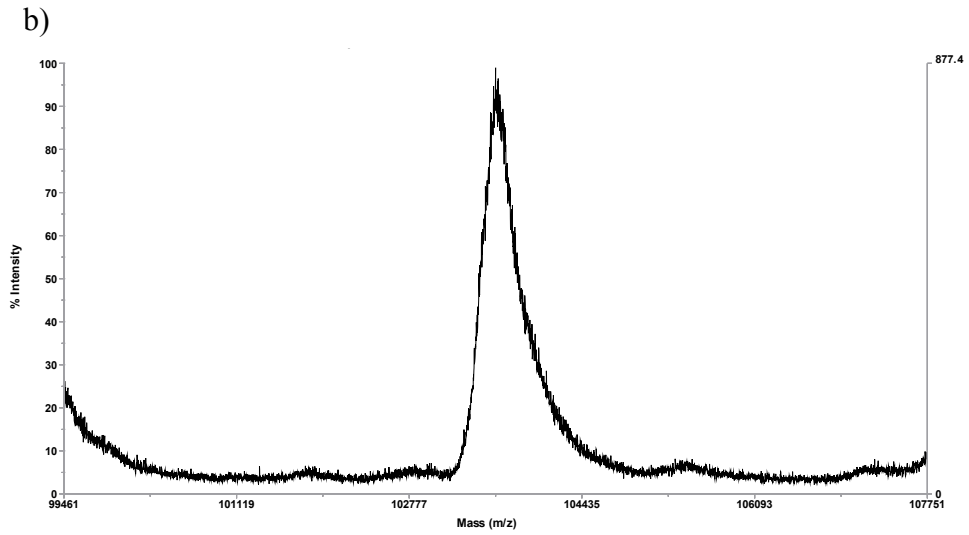
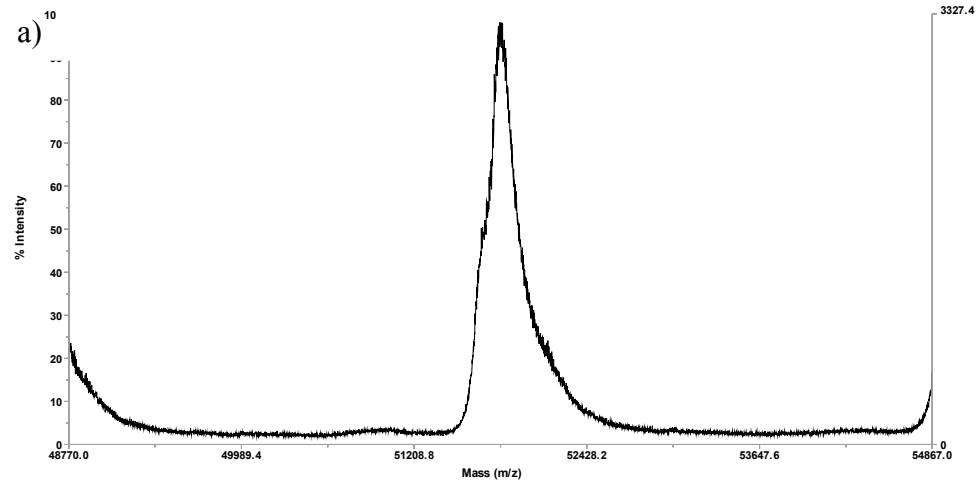
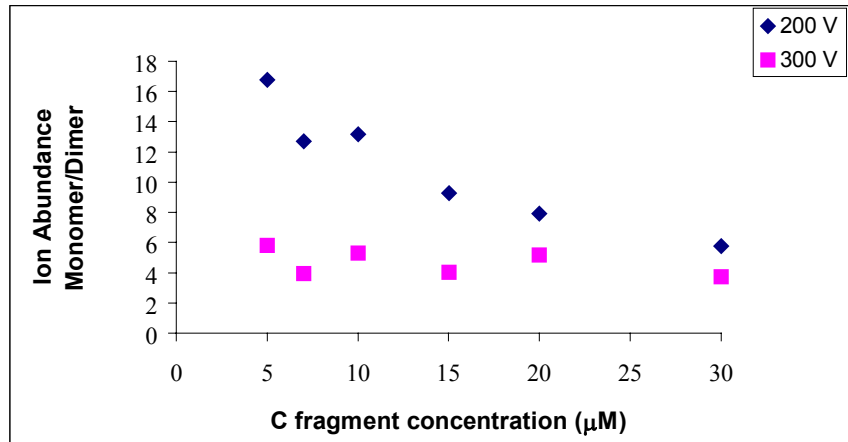
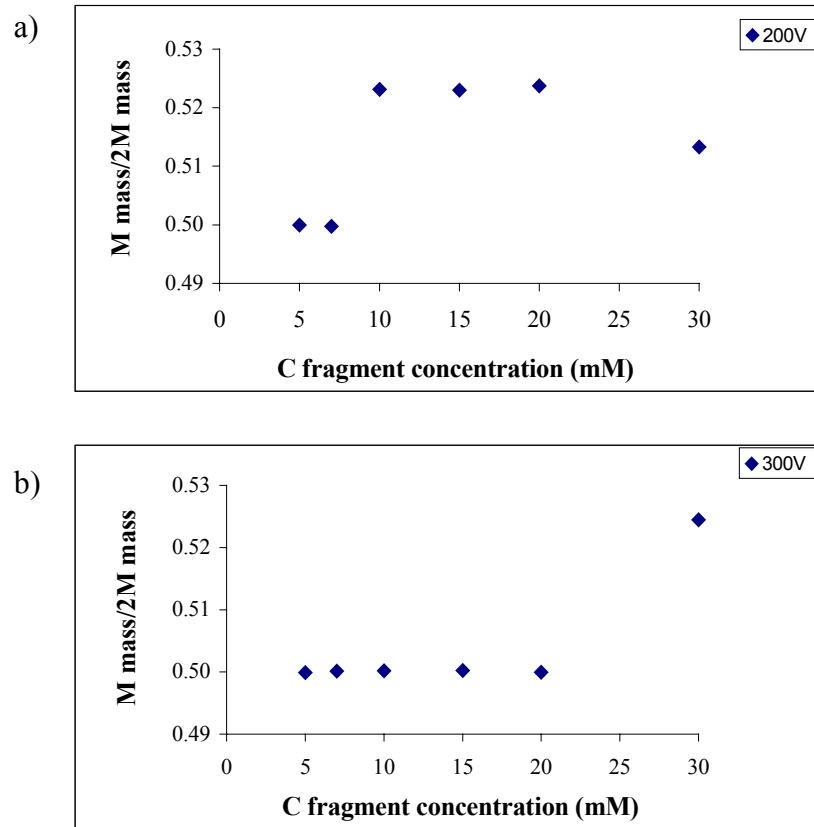


Figure 3. C fragment concentration vs. ion abundance of M/2M at declustering voltages of 200 and 300 V.



Tetanus C fragment μM	Declustering Potential	Monomer Ion Abundance	Dimer Ion Abundance
5	200	1375.7	82
7	200	2364.5	186
10	200	2220.5	168.8
15	200	1631.5	176.2
20	200	793.1	99.9
30	200	637.1	110.7
5	300	2492.2	430
7	300	3282.3	835.6
10	300	1805.7	341.7
15	300	2414.1	600.6
20	300	850.4	164.1
30	300	1529.8	411.4

Figure 4. Variation in the M/2M ratio of observed mass values after deconvolution, plotted against increasing C fragment concentration, at declustering voltages of a) 200 V and b) 300 V.



Tetanus C fragment $\mu\text{M}$	Declustering Potential	Monomer Mass Deconvolution	Dimer Mass Deconvolution
5	200	51818.9	103652.9
7	200	51812.4	103682.2
10	200	51855.2	99121.8
15	200	51858.9	99163.4
20	200	51978.3	99247.5
30	200	48623.2	94726.3
5	300	51812.5	103646.7
7	300	51818.8	103605.6
10	300	51842.6	103646.7
15	300	51855.2	103659.3
20	300	51903.1	103812.6
30	300	52015.9	99177.2

Figure 5. ESI MS spectra of the tetanus C fragment in, a) 10% methanol, showing both M and 2M peaks, and b) 40% methanol, showing the disappearance of the 2M peak. The protein concentration was 8.6  $\mu\text{M}$  in 3 mM ammonium acetate, pH 7.5. The declustering voltage was 200 V in both cases.

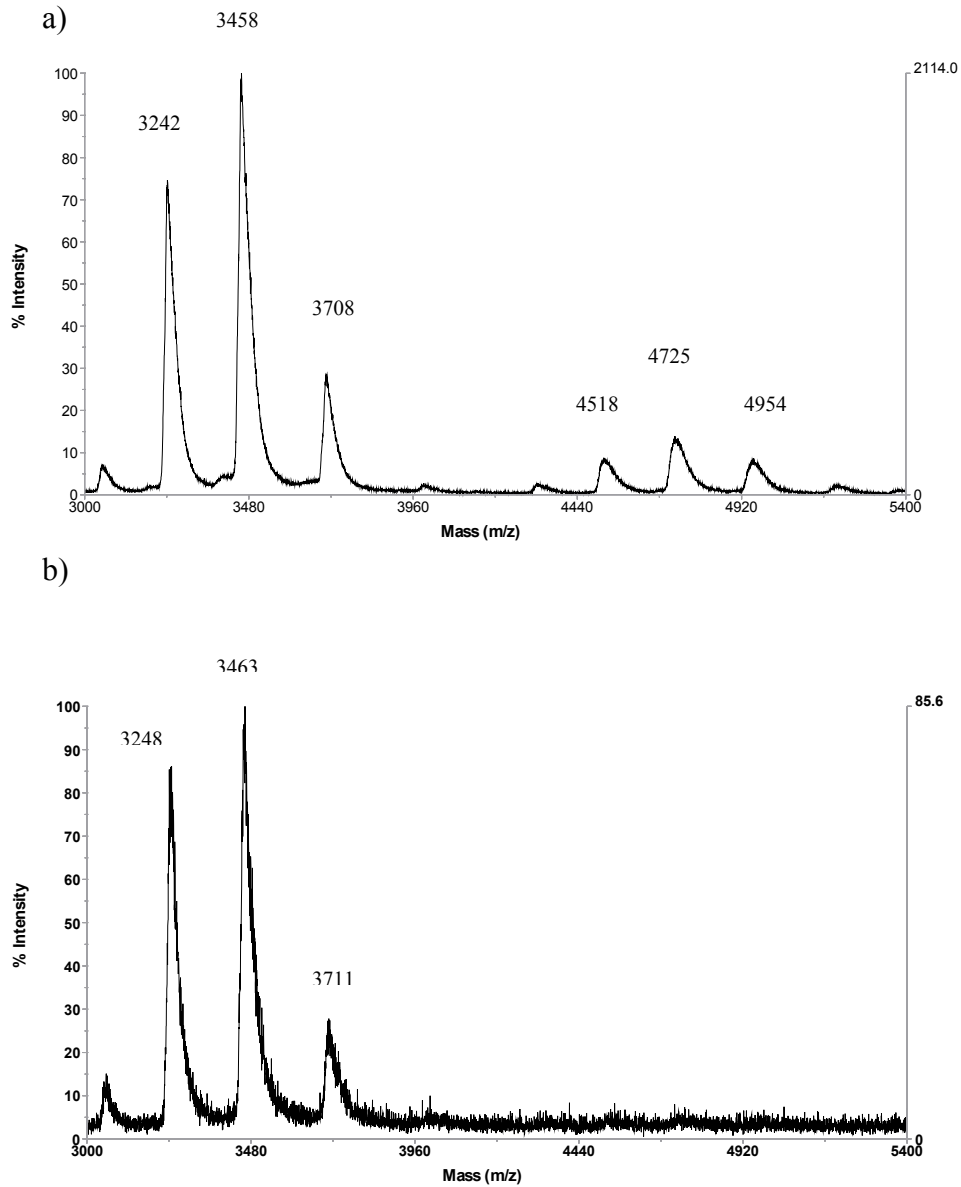


Figure 6. Deconvoluted spectra recorded with a declustering voltage of 200 V, showing complex formation between the C fragment and NeuAc dimers and trimers. a) Top trace, 1:4 C fragment : (NeuAc)<sub>2</sub>, bottom trace, 1:8 C fragment : (NeuAc)<sub>2</sub>. b) Top trace, 1:3 C fragment : (NeuAc)<sub>3</sub>; bottom trace, 1:7 C fragment : (NeuAc)<sub>3</sub>.

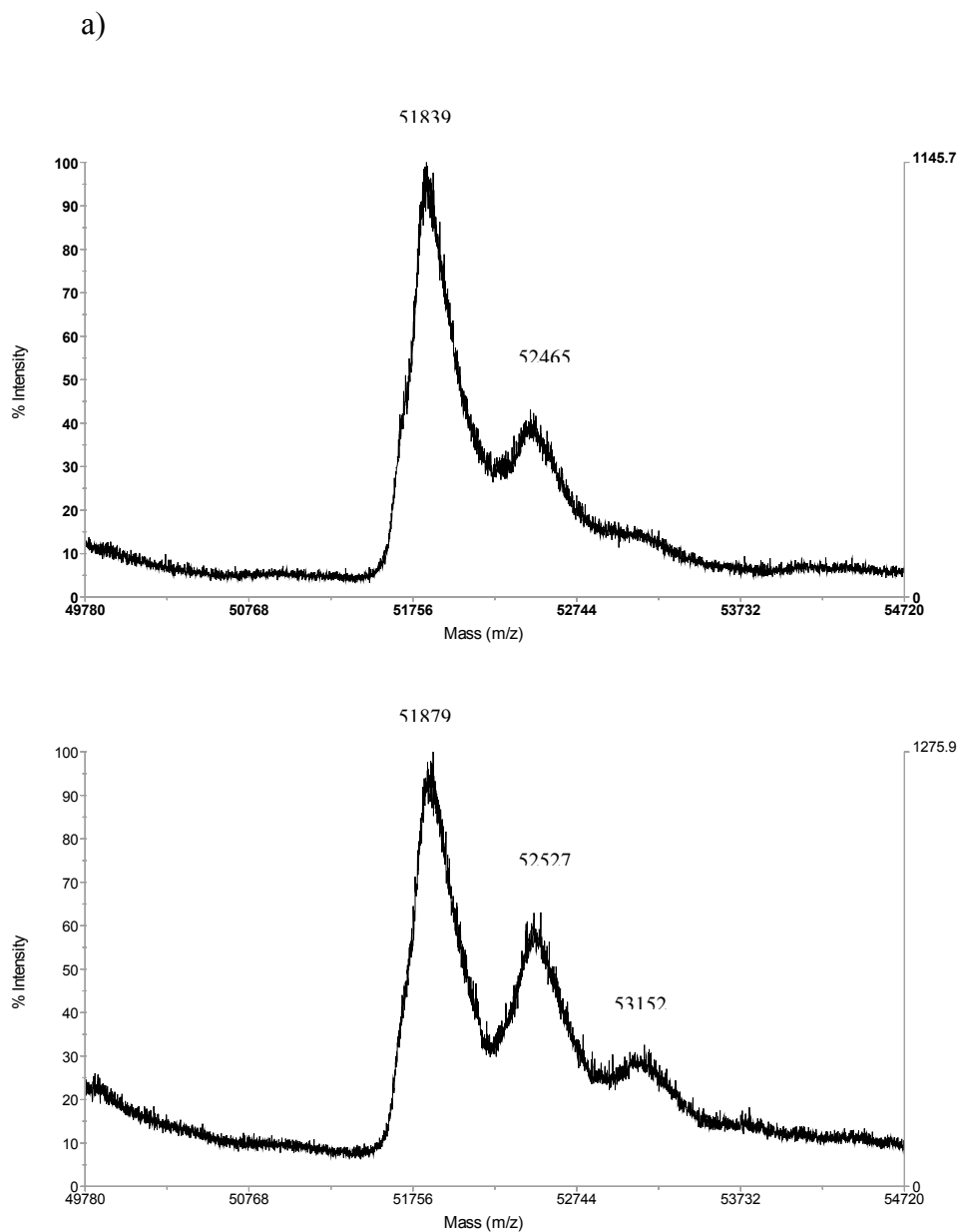


Figure 6. (continued)

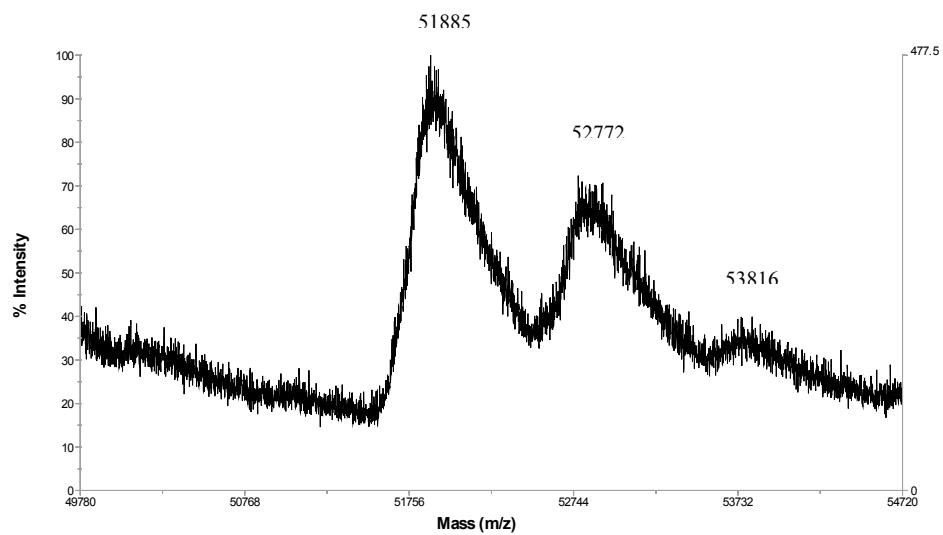
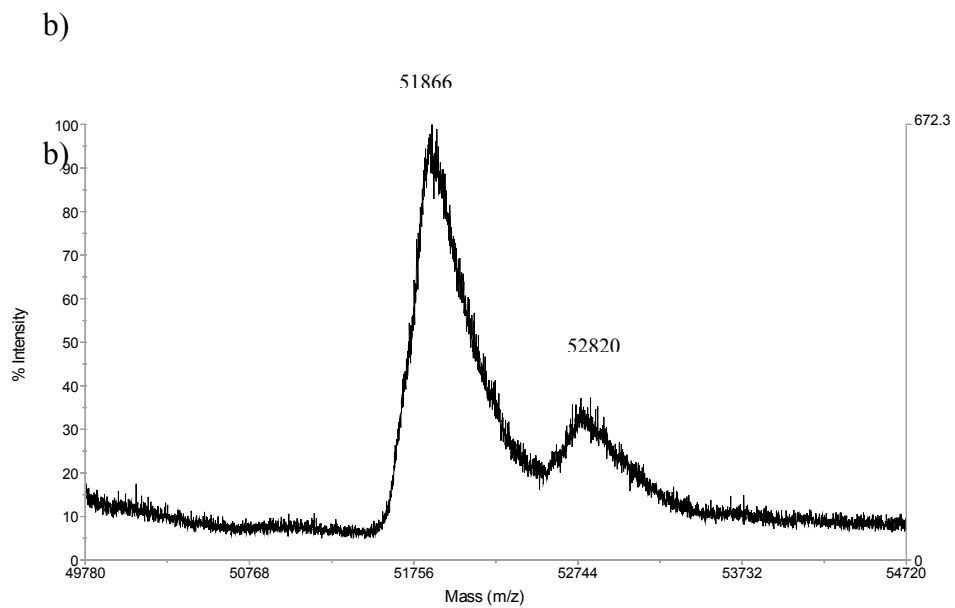


Figure 7. Binding of (NeuAc)<sub>3</sub> to the C fragment. The dissociation constant  $K_D$  is derived from the slope of the plot of the ratio of unbound C fragment/bound C fragment vs.  $1/[(\text{NeuAc})_3]$  (see equation 2).

